











# Highly Shape-Adaptable Honeycomb Gripper Using Orthotropic Surface Tension

Yong-Sin Seo , Jae-Young Lee , Chanhun Park , Jongwoo Park , Byung-Kil Han ,  
Je-Sung Koh , *Member, IEEE*, Uikyum Kim , *Member, IEEE*, Hugo Rodrigue , *Senior Member, IEEE*,  
Jeongae Bak , and Sung-Hyuk Song 

## I. INTRODUCTION

**Abstract**—Astrictive-type grippers, which generate gripping forces from adhesive forces at the contact surface, such as suction cup, are popular end-effectors as picking solutions because of their simplicity and small working space. However, the adhesive force of the astrictive gripper decreases with increasing complexity of the object surface; thus, its application has been restricted to simple picking of objects with a flat surface. Here, in this article, we present an all-round honeycomb astrictive gripper that has an orthotropic surface tension for grasping highly irregular shaped objects with an uneven surface. The design is inspired by mimicking the two-level (macro and mesoscale) shape adaptation of the octopus's leg. The stiffness-variable structure is also consisted to change its stiffness similar to the function of octopus's leg, and owing to the combination of these structures makes possible to perform various tasks, including hammering, breakfast serving, and vaccination, which were not possible for previous astrictive gripper.

**Index Terms**—Shape-adaptive structure, soft robotics, stiffness-variable structure, suction gripper, universal gripper.

Manuscript received 7 February 2023; accepted 20 March 2023. Date of publication 11 April 2023; date of current version 14 September 2023. This work was supported by a Grant of the Basic Research Program funded by the Korea Institute of Machinery and Materials under Grant NK239C, in part by a Major Project of the Korea Institute of Machinery and Materials under Grant NK244F, and in part by R&D Program (KEIT No. 20012602) of the Ministry of Trade, Industry and Energy, Korea Government. (*Corresponding author: Sung-Hyuk Song.*)

Yong-Sin Seo and Jae-Young Lee are with the Department of Robotics and Mechatronics, Korea Institute of Machinery and Materials, Daejeon 34103, South Korea, and also with the School of Mechanical Engineering, Sungkyunkwan University, Suwon 16419, South Korea (e-mail: sys7668@kimm.re.kr; leeje@kimm.re.kr).

Chanhun Park, Jongwoo Park, Byung-Kil Han, Jeongae Bak, and Sung-Hyuk Song are with the Department of Robotics and Mechatronics, Korea Institute of Machinery and Materials, Daejeon 34103, South Korea (e-mail: chpark@kimm.re.kr; jekiel@kimm.re.kr; bkhan@kimm.re.kr; jabak@kimm.re.kr; shsong@kimm.re.kr).

Je-Sung Koh and Uikyum Kim are with the Department of Mechanical Engineering, Ajou University, Suwon 16499, South Korea (e-mail: jskoh@ajou.ac.kr; ukim@ajou.ac.kr).

Hugo Rodrigue is with the School of Mechanical Engineering, Sungkyunkwan University, Suwon 16419, South Korea (e-mail: rodrigue@skku.edu).

This article has supplementary material provided by the authors and color versions of one or more figures available at <https://doi.org/10.1109/TIE.2023.3265032>.

Digital Object Identifier 10.1109/TIE.2023.3265032

**G**RIPPER was developed to allow robots to accomplish a specific task of handling target objects. These grippers can be categorized into four types: impactive, ingressive, astrictive, and constitutive grippers [1]. Among these, the most widely used grippers in the industry are impactive-type grippers, which use a direct mechanical force applied from two or more directions on the object using fingers or clamps, and astrictive-type grippers, which use an attractive force applied from the gripper using vacuum suction, magnetoadhesion, or electroadhesion [2]. The impactive-type gripper is commonly used for stable grasping of an object at a precise position [3], [4], [5], [6], [7]. Particularly, a soft finger-type gripper was developed for handling fragile objects, such as fruits and mushrooms. Pneumatic soft finger actuators for handling fried chicken, sushi, or mushrooms [8], [9]; origami ball-shaped contractible structures for handling various fragile objects [10]; and flexible rib structures with sensors for reorienting wine glasses [11] were proposed. However, these impactive-type grippers require sufficient side space for stable contact with the object to apply the force, and the force applied from each tip must be balanced when the object has oblique or complex side surface. On the other hand, astrictive gripper has the advantage of its simple gripping mechanism. It uses the attraction force toward the gripper and not compression force applied on the object; there is no need to control the gripping force and calculate the force balance from the gripping tip as is required for an impactive gripper. Moreover, the astrictive gripper can grip the object using a relatively small area of the target object compared with the impactive gripper [12] because only the top surface of the object contacts and adheres to the gripper [13], [14]. Because of these advantages, various types of astrictive grippers have been developed; they can be generally categorized into the following categories—vacuum suction, electroadhesion, magnetoadhesion, and gecko-like adhesion—depending on the source of the attraction force [1], [2], [15], [16]. The characteristics of each type of astrictive gripper are explained in the Supplementary text 1. Among astrictive grippers, the vacuum suction gripper is the most commonly used because of its advantages [17], but it requires a sealed area between the gripper and the surface of the target object to maintain a negative pressure; otherwise, the gripping force drastically decreases [18]. Therefore, if the suction cup or sponge

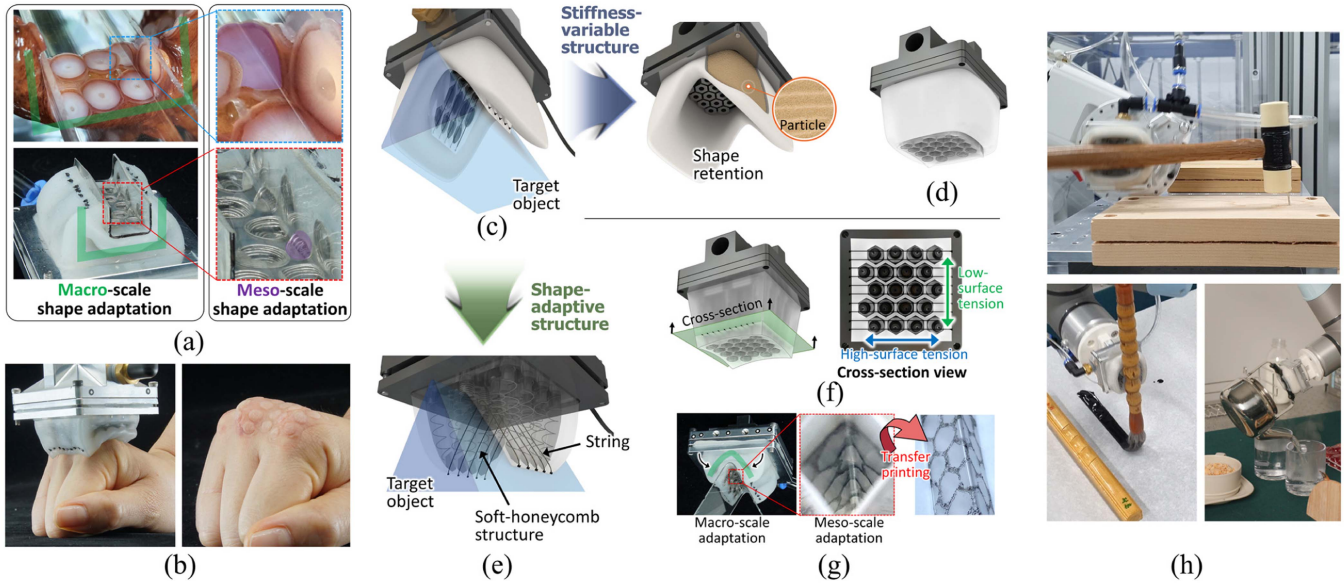


**Fig. 1.** Configuration of the honeycomb suction gripper (supplementary video 1). (a) Comparison of the shape adaptation of an octopus's leg with that of the honeycomb suction gripper at the macro- and mesoscales. (b) Remaining marks on the hand after the attached honeycomb suction gripper were removed. (c) Configuration of the adapted shape of the gripper for a triangular pillar structure. The right side of the photograph shows the stiffness-variable structure only without the shape-adaptive structure. (d) Initial shape of the gripper showing assembled components of the stiffness-variable structure and shape-adaptive structure. (e) Deformed shape of the shape-adaptive structure only. (f) Detailed configuration of the shape-adaptive structure (cross-sectional view). (g) Macro- and mesoscale shape adaptation with ink transfer printing. (h) Image of actual gripping shape of various objects and performing tasks—hammering (Supplementary video 9), calligraphy (Supplementary video 10), and preparing breakfast (Supplementary video 11).

structure cannot perfectly cling to the surface because of a complex surface shape, air leakage can occur through holes, grooves, or contact surfaces that are smaller than the gripper, and the gripping force decreases. To overcome these limitations, an origami mechanism was applied to realize a reconfigurable suction gripper using SMA wire as the actuating source [18]. The shape of this gripper can be changed into three modes based on the shape of the object to minimize leakage. However, the gripping force was less than 5 N, which was not sufficient for various applications, and the shape of the gripper should be controlled by an actuator. A gripper mimicking the suction cup of the octopus using a dielectric elastomer [19], shape memory alloy [20], particle jamming [21], micrometer-scale dome structures [22], four independent chamber structures [23], deployable spring structures [24], and biomimetic cupped microstructures [25] was implemented to increase the gripping force. A suction cup combined with a leg actuator mimicking the octopus was also presented. It was capable of wrapping the target object to increase the adhesion area of a rounded object [26]. These suction grippers gripped various types of objects. However, the surfaces of most gripping objects were flat, smooth, or gentle curvature. Hence, the previously developed suction gripper was limited in gripping objects with grooves, bumps, steps, and holes, which are the major barriers for suction grippers in the industrial field. Moreover, vacuum suction gripper cannot perform complex tasks because of low gripping force for uneven surface conditions and unstable—unpredictable gripping position for applied external force. However, these two limitations of a suction gripper are rather an advantage of an impactive gripper.

Therefore, there is a need for a new type of gripper that has the advantage of the two major types of grippers: impactive and astrictive grippers.

In this study, we present a universal honeycomb suction gripper that can grasp various objects with bumps, grooves, holes, and complex shapes, and even objects smaller than the gripper, which are technical barriers to the previous suction-type grippers, by mimicking the two-scale shape adaptation of the octopus. In addition, this honeycomb suction gripper can hold objects firmly enough to perform complex tasks using a stiffness-variable structure, which is the advantage of an impactive gripper, by mimicking the stiffness variation of the octopus. Therefore, the developed suction gripper combines the advantages from each gripping category: an astrictive gripper for using the minimum required area for gripping, and an impactive gripper for generating a high gripping force for a stable-firm grip. Owing to these distinctive features, the gripping force of the developed gripper is significantly improved compared with that of the existing commercialized universal suction grippers; furthermore, the gripper can perform complex tasks, such as hammering, calligraphy, serving breakfast, and vaccination.

## II. DESIGN AND MECHANISM OF THE GRIPPER

### A. Overall Configuration of the Honeycomb Structure

The soft honeycomb gripper can change its shape according to the shape of the target object via a two-level shape adaptation mechanism (see Fig. 1(a), Supplementary video 1). First, the macroscale shape adaptation allows shape deformation

according to the overall shape of the target object, such as a rectangular, triangular, or circular shape. While the macroscale adaptation maximizes the contact area to enclose the contour of an object, mesoscale adaptation causes deformation according to the detailed shape of the object, such as the edge of the rectangular prism, round surface of a circular object, or irregular rough surface of the object. This mesoscale adaptation minimizes air leakage at the contact surface between the gripper and object by adapting each soft hexagonal hole to the mesoscale contour of the object. Both macro- and mesoscale adaptations are simultaneously used and are both important, as can be observed from the gripping method of the leg of the octopus. When an octopus grabs an object, such as a rectangular prism, it wraps its leg around the prism; in this process, the shape of the legs adapts and is deformed according to the approximate contour of the prism, as shown by the green line in Fig. 1(a). Simultaneously, each sucker of the octopus adapts to the detailed shape of the object, such as the edge of the rectangular prism, as shown in the purple area in Fig. 1(a), which results in an effective, high adhesion force. The soft honeycomb gripper also follows a similar method to that followed by the octopus for effectively gripping the rectangular prism, macroscale shape adaptation of the overall structure to the prism, and mesoscale shape adaptation of each hexagonal hole to the edge of the prism. Because of these adaptation mechanisms similar to the octopus, a soft honeycomb gripper can generate an effective adhesion force even for the knuckle of the human hand, which has a large height variation and a complex shape; thus, clear marks due to the properly adhered holes can be observed [see Fig. 1(b)], such as the marks from the suckers of the octopus.

The honeycomb gripper consists of two major components: a shape-adaptive structure and a stiffness-variable structure [see Fig. 1(c)]. The shape-adaptive structure consists of a honeycomb structure that can change its shape according to the contour of the object. To increase the adaptability at the macroscale, we use an orthotropic structure, which has different tension at the top surface of honeycomb structure in its direction. The tension at top surface of the honeycomb structure is defined as the term “surface tension.”

In order to realize this orthotropic “surface tension,” multiple strings were used in the gripper. When the gripper comes in contact with a triangular shape perpendicular to the string orientation, the honeycomb structure effectively encloses the target object owing to the high surface tension [see Fig. 1(e)]. Ten strings are layered in parallel with each other [see Fig. 1(f)] and generate effective enclosing for the convex-shaped object at the macroscale. At the mesoscale, each hole in the honeycomb structure can be adapted to the edge of the triangle [see Fig. 1(g)]; therefore, all of the honeycomb holes can be fully contacted to the structure, including the edge side, as shown in the stamp transfer printing image, which shows a clear stamped line of each honeycomb hole. Therefore, it can generate a high adhesion force. The stiffness-variable structure helps hold the position of the gripped object even when an additional external force is applied to the object. The stiffness of the stiffness-variable structure is set to be low in the initial state, so it can be easily deformed according to the shape of the target object when

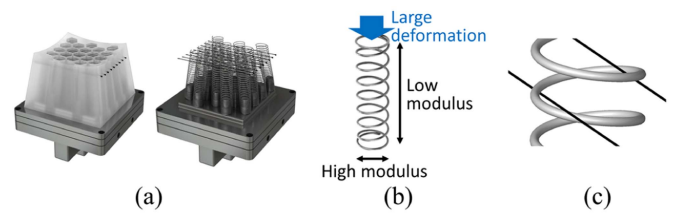


Fig. 2. Configuration of shape-adaptive structure. (a) Assembled state of the shape-adaptive structure on the left, and the configuration of the spring and string structure on the right. (b) Spring structure with different moduli in the longitudinal and lateral directions. (c) Assembly of the string and spring structures.

the object is pushed against the gripper. After the process of deformation is completed, the stiffness of the stiffness-variable structure increases, and the deformed shape of the structure can be fixed even when the object is removed from the structure [see right side of Fig. 1(c)]. Owing to the stiffness-variable structure, the developed gripper can perform not only simple picking tasks but also complex tasks, such as assembly and handling of tools. For example, the developed gripper can grip an object with a rough surface and large curvature in a stable manner, and it is possible to perform tasks, such as hammering with a hammer with a complex handle shape, calligraphy, and pouring hot water with kettle [see Fig. 1(h)].

### B. Configuration of the Honeycomb Structure With Orthotropic Surface Tension

Based on the polymeric honeycomb structure, the spring and string structure were placed at honeycomb structure [see Fig. 2(a), Supplementary Fig. 1]. The spring structure plays a role in maintaining the air flow passage due to its high modulus in the lateral direction. At the same time, the spring structure can be easily deformed at the vertical direction, which is required for effective shape adaptation [see Fig. 2(b)]. The dimensions of the spring structure were 5, 4, and 25 mm for the external and internal diameter, and the free length, respectively. The modulus of the spring structure was 22.7 kPa and 3.05 MPa in the vertical and lateral direction, respectively. The position of the spring structure can be held by the string structure because the two strings pass through each spring structure on both sides [see Fig. 2(c)]. In the combined state with the honeycomb structure and string, the measured modulus was 120.7 kPa.

In case of string structure, it was placed at the honeycomb structure to effectively grip convex-shaped objects, as described in Section II-A. Each string is sufficiently thin so that the surface tension of the honeycomb structure in the vertical direction to the direction in which the string is placed is the same as that before the string is embedded. In contrast, the surface tension of the honeycomb structure in the direction parallel to the direction in which the string is embedded is increased owing to the string structure. Therefore, the honeycomb structure exhibits orthotropic surface tension characteristics according to the string orientation. This orthotropic surface tension can be effectively used to grip a complex-shaped object. In the case of a convex-shaped object, the gripper can effectively enclose the

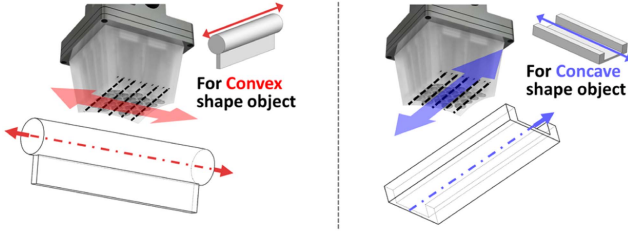


Fig. 3. Gripping orientation for a convex-shaped and concave-shaped object.

target object when the object is pushed against the perpendicular direction of the string structure owing to the high surface tension (see Fig. 3). Otherwise, in the case of a concave-shaped object, the gripper can be effectively deformed when the object is pushed against the parallel direction of the string structure due to the effective surface elongation from its low surface tension.

These deformation characteristics according to the relative orientation between the longitudinal axis of the object and string structure were analyzed as follows. In the initial state of the high surface tension case, when the object pushed perpendicularly to the direction of string alignment, the honeycomb structure could be simplified as a rectangle, as shown in the right side of Fig. 4(a). In this model, the relation between the string and deformation angle of the gripper was mainly focused to be evaluated. Hence, the magnitude of the external force applied to the gripper was not considered. Only the external thick-wall structure and length of the string were considered, excluding the inner honeycomb structure consisted by low-modulus thin-wall structure. The location of the string was assumed as the top of the honeycomb structure, and its initial length was  $2\ell_{s\_int}$ . The initial height of the honeycomb structure was  $\ell_p$ , and its length was assumed to be constant during deformation. The bottom fixed length of the honeycomb structure was  $2a$ . After the indenter rods were pushed down, as shown in the left side of Fig. 4(b), the deformation of the right and left sides of the structure was assumed to be the same, so the only right side of the structure is shown in right side of Fig. 4(b). The deformation magnitude was assumed such that the indenter was pressed down to the bottom of the honeycomb structure. Then, the location of the edge of the honeycomb structure, which is represented as  $(y_1, z_1)$ , can be described as follows.

$$z_1 = \sqrt{\rho^2 - (y_1 + (\rho - a))^2} \quad (1)$$

where  $\rho$  is the radius of curvature for the deformed shape of the outside contour of the honeycomb structure. In this analysis, the deformation contour of side wall of the honeycomb structure has a constant curvature. Furthermore,  $\theta$  is the angle of the deformed top surface of the honeycomb structure. Additionally,  $\ell_s$  is the elongated length of string, and its elongation ratio  $k$  is given as follows:

$$\ell_s = (k + 1) \ell_{s\_int} \quad (2)$$

where  $k$  is used as a variable parameter to show the deformation characteristics in this model, not the measured value.

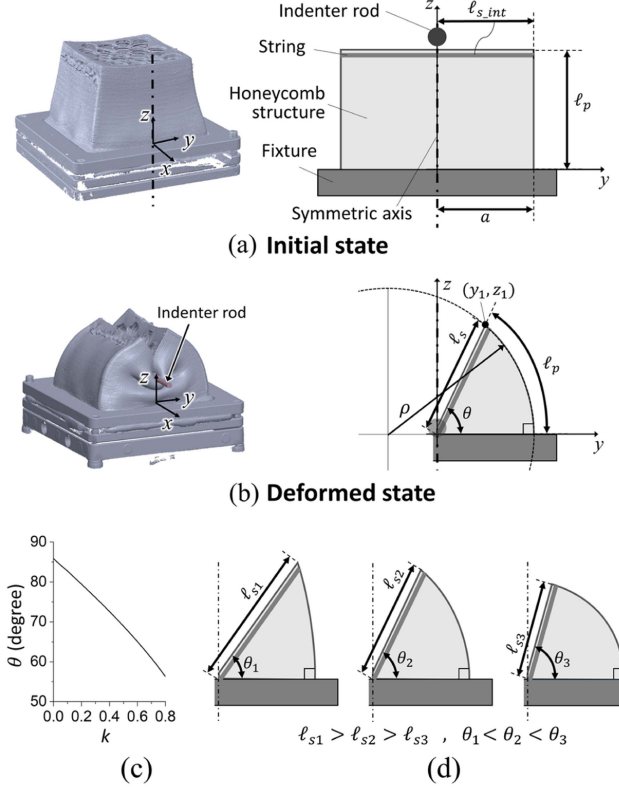


Fig. 4. Analysis of deformation characteristics according to the elongation ratio of string for gripping convex-shaped object. (a) Initial state of the honeycomb structure. (b) Deformation of the honeycomb structure as the indenter rod is pressed in the center position. (c) Expected variation of the deformation angle according to the elongation ratio  $k$ . (d) Deformation shape of the honeycomb structure according to the elongated length of string.

Then,  $y_1$  and  $z_1$  are described as follows:

$$y_1 = \frac{((k + 1) \ell_{s\_int})^2 + a^2 - 2\rho a}{2(a - \rho)}$$

$$z_1 = \sqrt{((k + 1) \ell_{s\_int})^2 - \frac{((k + 1) \ell_{s\_int})^2 + a^2 - 2\rho a}{2(a - \rho)}} \quad (3)$$

From (3), the angle  $\theta$  can be described as follows:

$$\theta = \tan^{-1} \left[ \sqrt{\left( \frac{2(k + 1)(a - \rho) \ell_{s\_int}}{((k + 1) \ell_{s\_int})^2 + a^2 - 2\rho a} \right)^2 - 1} \right] \quad (4)$$

The relationship between  $\rho$  and  $\theta$  also can be described as follows:

$$\frac{(k + 1) \ell_{s\_int}}{\sin \frac{\ell_p}{\rho}} = \frac{\rho}{\sin(\pi - \theta)} \quad (5)$$

From (4) and (5), the angle  $\theta$  can be derived from the variation of the elongation ratio  $k$ , as shown in Fig. 4(c), when  $a$  is 17.4 mm and  $\ell_p$  is 26.0 mm. The maximum value of  $k$  is 0.8 when the side wall of the structure is not bent and only the string is elongated. The angle increases as the elongation ratio of string decreases. This trend is described in Fig. 4(d). As the string does not stretch,

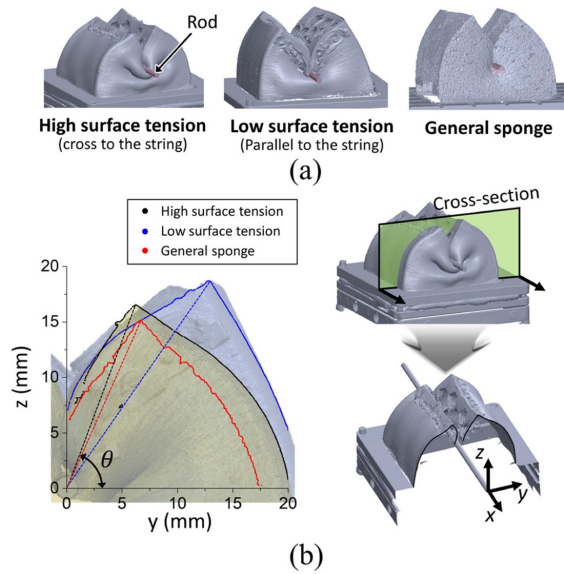


**Fig. 5.** Shape adaptation for simplified convex-shaped object depends on the characteristics of surface tension. (a) Deformation shape with the pole pressed at the center captured by a 3-D scanner. (b) Contour of each structure with an overlapped image of deformation (yellow: high surface tension and blue: low surface tension). The graph shows the measured point from the 3-D scanner located at the cross-sectioned plane described at the right side of the figure.

the deformation angle increases, and the amount of structural deformation increases, which means that the tension applied to the string also increases. As the deformation angle increases, it is advantageous for the gripping shape of a convex-shaped object, so high surface tension at the top surface of a structure can be appropriate for gripping a convex-shaped object.

### C. Mechanical Characteristics of Orthotropic Surface Tension of the Honeycomb Structure

To verify the effect of the orthotropic surface tension mechanism, we measured the deformation image of the honeycomb structure according to the relative orientation of the string structure using a 3-D scanner. First, the rod was pushed against the center of the honeycomb structure as a simplification of a situation where a convex-shaped object is pushed against the center of the gripper for gripping [see Fig. 5(a)].

To compare the magnitude of the converging deformation, we measured the position of the edge of the honeycomb structure and calculated the converging distance and angle after deformation [see Fig. 5(b)] using the cross-sectioned points of each structure. As the magnitude of the deformation at which the edge of the gripper converges in the inward direction increases, the probability of realizing a larger contact area between the gripper and convex-shaped object increases. In this respect, the case of high surface tension that shows largest deformation angle  $69^\circ$  and smallest distance 6.3 mm ( $y$ -axis) from the center is the most appropriate for gripping convex-shaped objects.

In the case of gripping a concave-shaped object, the both rods located at the edge of gripper were compressed, as shown in Fig. 6(a). To quantitatively compare the characteristics of each

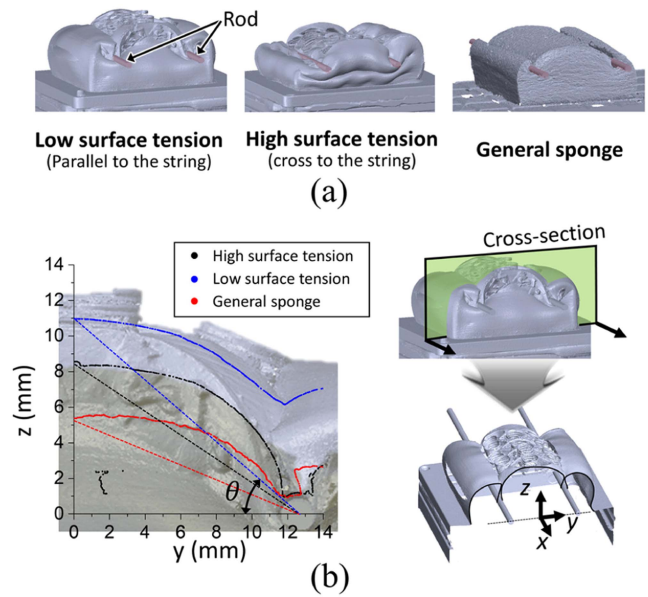


**Fig. 6.** Shape adaptation for simplified concave-shaped object depends on the characteristics of surface tension. (a) Deformation shape with the two poles pressed at the edge of structure captured using a 3-D scanner. (b) Contour of each structure with the overlapped image of deformation (yellow: high surface tension and blue: low surface tension).

structure, the deformation angle and height of the middle part of the structure were measured, as shown in Fig. 6(b). The low-surface-tension case showed the largest angle of  $40^\circ$  and middle part height of 10.9 mm compared with others, so it can be concluded that it is appropriate for gripping concave-shaped objects.

## III. GRIPPING PERFORMANCE EVALUATION

### A. Macroscale Shape Adaptation

To verify the gripping performance of the gripper, we used three typical object shapes (rectangular prism, triangular prism, and cylindrical shape) to measure the gripping force by changing the size of each object (Fig. 7, Supplementary Figs. 2–5, Supplementary videos 2–4). The initial pressing force required to realize shape adaptation was set to 20 N in this experiment. The resultant range of the pressing distance varied based on the shape of the object, but it was in the range of 15–17 mm. The high surface tension case in which the string in the honeycomb structure is aligned across the axial axis of the target object shows higher gripping weight compared with the low-surface-tension case and a general suction cup commercially used for gripping complex-shaped plastic bags (SPB1 30 ED-65 SC040, Schmalz, size  $\phi 33$  mm). In the case of the concave-shaped structure, the low-surface-tension case shows the higher gripping weight compared to the other cases, as predicted in Section II.

When the gripper is positioned at the offset of the object center, the gripping ability generally decreases compared to that in the well-aligned situation. However, this can occur in real circumstances owing to the inaccurate vision system. Therefore, we verified the gripping ability of an offset-positioned object from the centerline with a convex-shaped object (see Fig. 7(c),

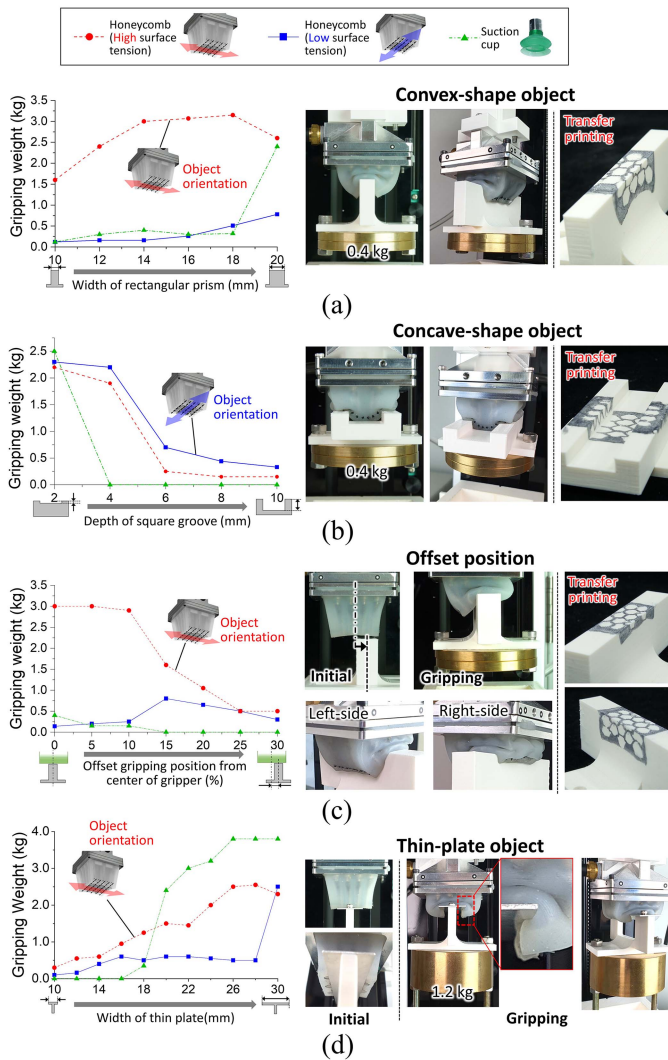


**Fig. 7.** Measurement of gripping weight for macroscale adaptation. (a) Comparisons of gripping weight depend on the gripper characteristics and the suction gripper for convex-shaped objects. (b) Concave-shaped object, the offset-positioned object, and (d) thin-plate objects.

Supplementary Fig. 4, Supplementary video 4). In the case of high surface tension, the gripping weight remains unchanged until the offset value is 10%, owing to the enclosing deformation around the target object.

The characteristics of high surface tension in the honeycomb structure combined with the soft material can also generate enclosing deformation for the thin-plate shape [see Fig. 7(d)]. Even when the width of the plate is smaller than the width of the honeycomb structure (34.8 mm), the edge side of the hexagonal hole is not fully blocked by the object, and a high gripping force can be realized by hooking the edge of the thin plate. Because of this, the high surface tension case shows a higher gripping weight than the lower surface tension case. The reason the suction cup shows higher gripping force when the width of the thin plate exceeds 20 mm is because of the geometric characteristics of suction cup used in the experiment (Supplementary Fig. 6)

For a gripping object comprising a hyperelastic material, the gripper also exhibited a force similar to that of an object comprising a rigid material (Supplementary Fig. 8). The low-surface-tension case also exhibited a high gripping force for a convex-shaped hyperelastic object because of the shape adaptation of the target object itself.

To verify the effect of the contact between the honeycomb structure and target object, the gripper surface was covered with ink; we reproduced the gripping sequence to the target object and checked the transferred ink from the gripper surface to the object surface. As seen on the far right side of Fig. 7(a)–(d), the shape of each hexagonal hole was clearly transferred to the object surface even at the edge and vertical wall side. This means that each hexagonal hole can realize a sealed area without air leakage, and each hole provides a high vacuum pressure for a high and stable holding force.

## B. Mesoscale Shape Adaptation

A gripping force can be generated by the honeycomb structure even if the entire honeycomb structure does not adapt to the target object. The entire structure of the honeycomb is adaptable to the object owing to its softness and orthotropic surface tension characteristics; this is defined as macroscale adaptation. Moreover, each hexagonal hole in the structure is also adaptable to the target shape, which is defined as mesoscale adaptation. If the shape of each hexagonal hole is well adapted to the object, the gripping force can be uniformly realized regardless of the gripping position. This means that effective gripping can be realized regardless of where an object is positioned on the gripper, so it can be said to represent the gripping performance of the gripper well. To realize these characteristics, the wall structure comprising each hole was sufficiently thin and had the same thickness for its modulus. In addition, the shape of the hole must be similar to a circle rather than a triangle or rectangle to minimize the modulus nonuniformity at the vertices. In this regard, the honeycomb structure is advantageous because of its uniform compression modulus, thus realizing an effective mesoscale adaptation.

We measured the gripping force by changing the location of the target object to verify the location dependency of the gripping force using different object sizes (Fig. 8, Supplementary Fig. 9). In this experiment, the pressing distance was set as 15 mm, not compression force because the change in size of target object is too large than in the general case. The gripping force was generally higher at the center of the gripper than at the other positions. However, the deviation in the gripping force was not large, and this trend is maintained for all cases. This is because of the effective shape adaptation of each hexagonal hole to the target object [see Fig. 8(b) and (c)]. At the gripping force measurement in this section, the initial pressing distance was fixed as 15 mm for maintaining the consistency of experimental condition, but the gripping force also can be generated at even smaller pressing distance due to the effective shape adaptation (Supplementary Fig. 10).

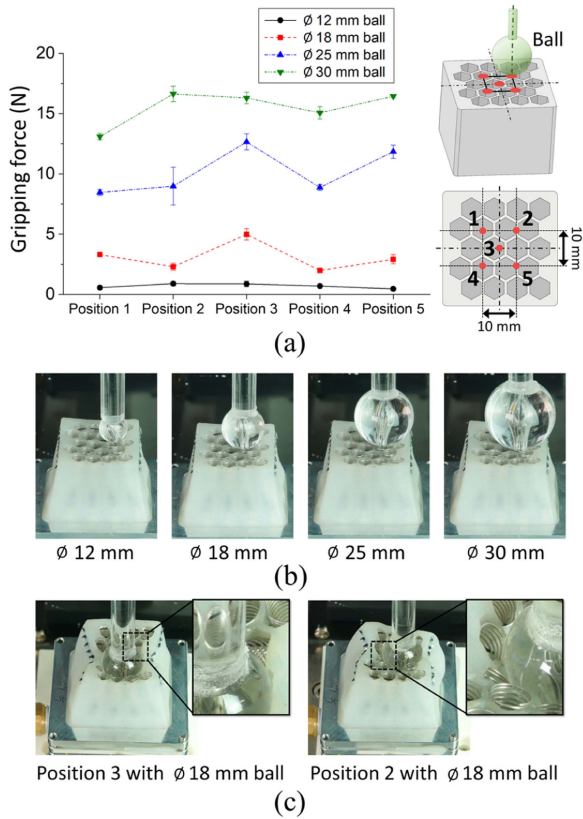


**Fig. 8.** Measurement of gripping force for mesoscale adaptation. (a) Gripping force depends on the relative position of the object to the gripper. (b) Size of each ball-shaped object was compared with the size of the honeycomb structure and displayed. Each object is located at position “2.” (c) Shape adaptation of the honeycomb structure to the ball object located at positions “2” and “3.”

Because of these shape adaptations, the cable gland with irregular shape could be successfully gripped in every orientation (Supplementary video 5).

#### IV. STIFFNESS-VARIABLE STRUCTURE FOR HOLDING THE GRIPPING POSITION

Most of the astrictive-type grippers cannot perform certain tasks except for simple picking and placing because of its low gripping force and low accuracy in positioning for gripping. These two limitations of the astrictive-type gripper make it difficult to maintain the gripping position and state when an additional external force is applied while performing a task. In this section, we describe the stiffness-variable structure to maintain the gripping position for increasing accuracy in gripping positioning and gripping stability.

This stiffness-variable structure has a square-shell shape, and the honeycomb structure is placed at the hollow area of the stiffness-variable structure. The stiffness-variable structure can change its stiffness in real time, and this function is similar to that of the octopus’s legs [see Fig. 9(a)] [27], [28], [29]. The octopus can change the stiffness of the arm to apply high forces by using combined contractions of muscles [30]. Similar to the octopus, the stiffness of the stiffness-variable structure consisted in the

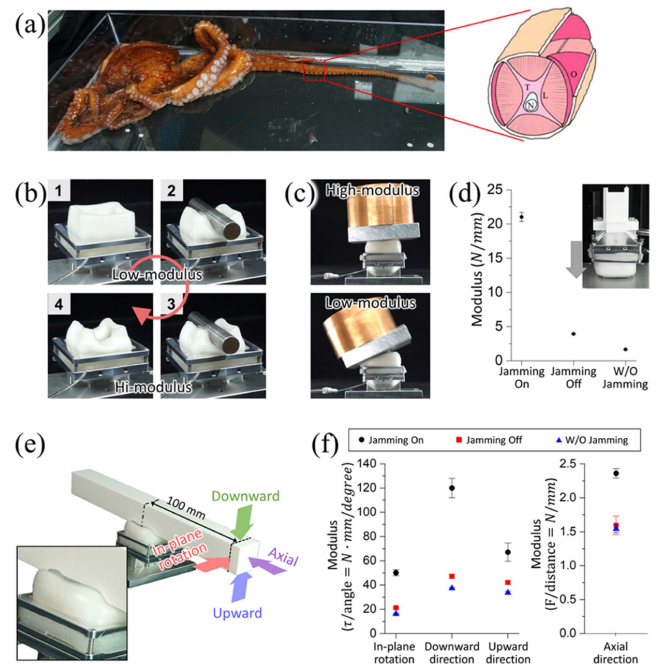


**Fig. 9.** Configuration of the stiffness-variable structure. (a) Stiffness-variable function of an octopus’s leg and the muscle structure for changes in stiffness. Right-side picture is from the article presented in [20]. (b) Shape retention of the stiffness-variable structure by changing the stiffness. (c) Weight supporting function of the stiffness-variable structure for the tilted condition. (d) Modulus variation in the jamming ON-state, jamming OFF-state, and without jamming state. (e) Experimental setup for evaluating the gripping position from the external force. Each arrow describes the direction of the applied force. (f) Rigidity of the gripping condition according to the direction of the applied force.

gripper (Supplementary Fig. 12) is increased to maintain the gripped position of the object [see Fig. 9(b)]. In the initial state, the stiffness-variable structure has a low modulus; therefore, its shape can be easily adapted according to the target object [second picture of Fig. 9(b)]. After shape adaptation is completed, the modulus of the stiffness-variable structure increases, and the stiffness-variable structure can hold the position of the object [third picture of Fig. 9(b)]. In the high-modulus state, the deformed shape can be maintained even when the gripped object is removed [fourth picture in Fig. 9(b)]. When the object is released, the modulus of the stiffness-variable structure returns to the original low-modulus state and then recovers its original square-shell shape.

Negative pressure was used to increase the modulus of the stiffness-variable structure, so the jamming mechanism [31] is activated as a compression force is generated from the polymeric wall structure to the particles enclosed inside the polymeric square-shell structure. This modulus variation of the stiffness-variable structure can effectively support the heavy weight, so it can reliably support the heavy weight (4 kg) in the high-modulus state even when it is tilted (upper side of Fig. 9(c), Supplementary video 6). When the modulus of the stiffness-variable structure changes from high to low, it can be seen that the weight cannot be supported and collapses [bottom side of Fig. 9(c)].

We measured the value of the modulus variation from the stiffness-variable structure [see Fig. 9(d)]. When a negative

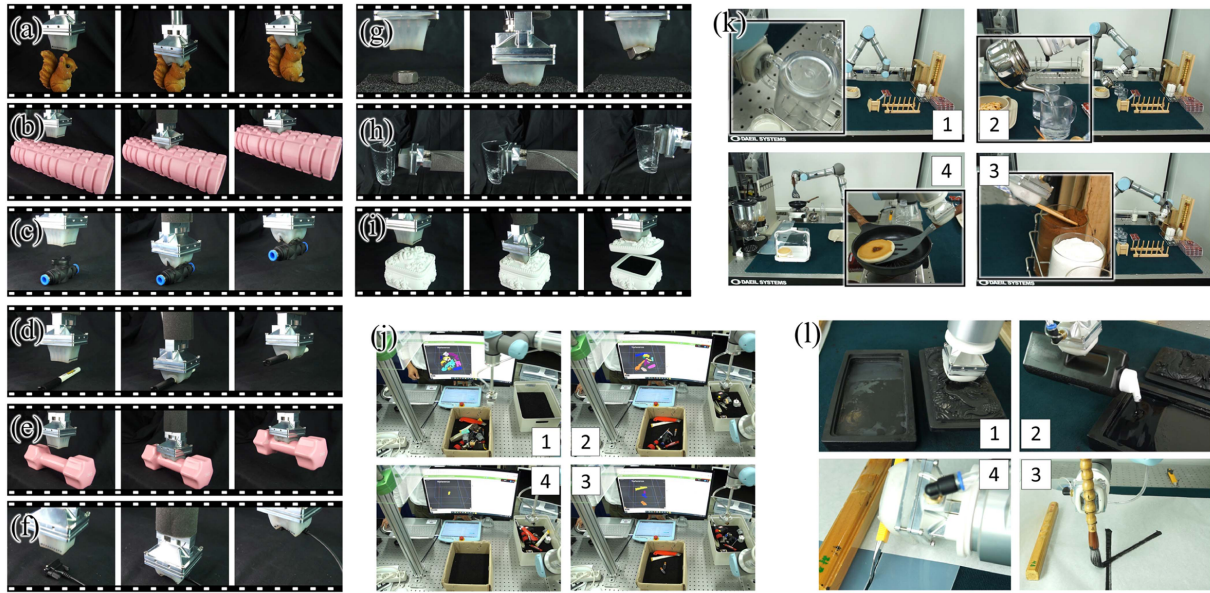


**Fig. 10.** Demonstration of gripping performance: Gripping of (a) squirrel model, (b) foam roller, (c) fitting valve, (d) pen, (e) dumbbell, (f) RGB cable gender, (g) nut, (h) heart-shaped cup, and (i) rose-sculptured jewellery box lid. (j) Bin picking of 14 types of unregistered 17 objects using a 3-D vision camera. (k) Preparing breakfast. (l) Writing calligraphy.

pressure is applied to the stiffness-variable structure and it changes to the high-modulus state, the modulus increases by 5.35 times compared with the low-modulus state.

A rectangular bar-shaped object was used as the target object to verify the ability of holding the gripping position [see Fig. 9(e)]. After the rectangular bar object is gripped by the gripper in the high-modulus state of the stiffness-variable structure, an external force is applied according to the four different directions, and the modulus is measured under each condition. As a result, the jamming ON-state showed a higher modulus for external forces applied to all directions by at least 1.39 times and at most 2.37 times compared with the jamming OFF-state [see Fig. 9(f)]. Therefore, it can be said that the dominant effect of the stiffness-variable structure was verified to hold the position of the gripped object.

## V. PRACTICAL APPLICATION

The picking ability of various daily life items that were especially difficult to grip using a traditional astrictive gripper was evaluated, as shown in Fig. 10(a)–(i) and Supplementary video 7. Based on this gripping performance, the bin picking of various objects was demonstrated using a vision camera (see Fig. 10(i), Supplementary video 8). The objects used in the bin picking were not registered in advance, so the vision system could only recognize the vague contour of an object without information regarding the surface or detailed contours. In addition, these objects were stacked on each other, so clear recognition of object orientation was difficult without machine learning. However, the developed gripper could grip the object with a complex shape-by-shape adaptation; therefore, the gripping strategies are not important for this demonstration. Thus, all stacked objects in the box could be successfully transferred to the other box. The

gripper can grip the handle of a hammer and hit the exact position of a nail multiple times (Supplementary video 9). The gripper also can stably grip a calligraphy brush, which has complex surface, and write the letters “KIMM,” which requires it to stably hold the calligraphy brush despite the repulsion force from the deflection of the brush due to the interaction between the brush and the paper (see Fig. 10(j), Supplementary video 10). The gripper not only writes the letter but also opens the inkstone, pours the ink, and cuts the paper with a box cutter. Furthermore, the gripper can prepare breakfast (see Fig. 10(k), Supplementary video 11), unplugging the electric plug from outlet and plugging it back into the outlet (see Fig. 10(l), Supplementary video 12), and perform a vaccination (Supplementary video 13).

## VI. CONCLUSION

In this article, an all-round suction-type gripper was presented capable of adapting to the contour of a target object at the macro- and mesoscales by mimicking the octopus’s leg to realize a stable and high gripping force even for irregularly shaped objects. To realize effective shape adaptation at the macroscale, similar to the octopus’s leg wrapped around the target object, an orthotropic surface tension mechanism was applied using a string structure. Also, each flexible hexagonal hole acts as octopus’s sucker, and it can effectively adapt to the edges or complex surfaces of the target object at the mesoscale. To maintain the gripping position, a stiffness-variable structure capable of changing its stiffness in real time was combined with the gripper, and we demonstrated complex tasks, such as calligraphy, preparing breakfast, hammering, and vaccination, which were difficult to perform using previous astrictive grippers.

However, the developed gripper exhibited the limitation of a relatively low gripping force for small and thin objects. The



gripper can grip these objects with mesoscale adaptation of several hexagonal holes, but the gripping force decreases due to air leakage from the other opened hexagonal holes. Therefore, an object, such as wire, which was smaller than the hexagonal hole or an object, such as mesh, which the air can pass through the surface was difficult to grip. The other limitation of the gripper was its lower gripping force for flat surfaces compared with the general suction cup. This trend becomes clearer as the surface of the target object approaches the flat plane, so this gripper was expected to be suitable for applications that require handling objects of various shapes.

As the future work, we aim to develop a mechanism to change the surface area of the gripper in real time so that it can grip thin and small objects. In addition, finite element method (FEM) analysis model to predict the deformation of the gripper will be developed based on the nonlinear large deformation and anisotropic material properties.

The developed shape-adaptable honeycomb suction gripper could lead to new possibilities of application of astrictive-type grippers as a multipurpose end-effector capable of performing various tasks, which was assumed to only be possible with impactive-type grippers, such as a parallel gripper or a high-DOF robot hand.

## REFERENCES

- [1] G. J. Monkman, S. Hesse, R. Steinmann, and H. Schunk, *Robot Grippers*. Hoboken, NJ, USA: Wiley, 2007.
- [2] K. Tai, A.-R. El-Sayed, M. Shahriari, M. Biglarbegian, and S. Mahmud, "State of the art robotic grippers and applications," *Robotics*, vol. 5, no. 2, 2016, Art. no. 11.
- [3] M. Grebenstein et al., "The hand of the DLR hand arm system: Designed for interaction," *Int. J. Robot. Res.*, vol. 31, no. 13, pp. 1531–1555, 2012.
- [4] G. Palli et al., "The DEXMART hand: Mechatronic design and experimental evaluation of synergy-based control for human-like grasping," *Int. J. Robot. Res.*, vol. 33, no. 5, pp. 799–824, 2014.
- [5] J.-Y. Lee et al., "Shape-adaptive universal soft parallel gripper for delicate grasping using a stiffness-variable composite structure," *IEEE Trans. Ind. Electron.*, vol. 68, no. 12, pp. 12441–12451, Dec. 2021.
- [6] J. Bohg, A. Morales, T. Asfour, and D. Kragic, "Data-driven grasp synthesis—A survey," *IEEE Trans. Robot.*, vol. 30, no. 2, pp. 289–309, Apr. 2014.
- [7] J.-K. Oh, S. Lee, and C.-H. Lee, "Stereo vision based automation for a bin-picking solution," *Int. J. Control, Autom. Syst.*, vol. 10, no. 2, pp. 362–373, 2012.
- [8] Y. Yamanaka, S. Katagiri, H. Nabae, K. Suzumori, and G. Endo, "Development of a food handling soft robot hand considering a high-speed pick-and-place task," in *Proc. IEEE/SICE Int. Symp. Syst. Integr.*, 2020, pp. 87–92.
- [9] J. Rong, P. Wang, Q. Yang, and F. Huang, "A field-tested harvesting robot for oyster mushroom in greenhouse," *Agronomy*, vol. 11, no. 6, 2021, Art. no. 1240.
- [10] S. Li et al., "A vacuum-driven origami 'magic-ball' soft gripper," in *Proc. Int. Conf. Robot. Autom.*, 2019, pp. 7401–7408.
- [11] S. Q. Liu and E. H. Adelson, "GelSight Fin Ray: Incorporating tactile sensing into a soft compliant robotic gripper," in *Proc. IEEE 5th Int. Conf. Soft Robot.*, 2022, pp. 925–931.
- [12] G. Mantriota, "Theoretical model of the grasp with vacuum gripper," *Mech. Mach. Theory*, vol. 42, no. 1, pp. 2–17, 2007.
- [13] Schmalz, "Gripping system for bin-picking applications (SBPG-SET X QS 50)." Accessed: Aug. , 2022. [Online]. Available: <https://www.schmalz.com/en572kr/vacuum-technology-for-robotics/handling-sets/bin-picker-sbpg-323551/10.01.45.00012>
- [14] J. Mahler, M. Matl, X. Liu, A. Li, D. Gealy, and K. Goldberg, "Dex-Net 3.0: Computing robust vacuum suction grasp targets in point clouds using a new analytic model and deep learning," in *Proc. IEEE Int. Conf. Robot. Autom.*, 2018, pp. 5620–5627.
- [15] S. Song, C. Majidi, and M. Sitti, "GeckoGripper: A soft, inflatable robotic gripper using gecko-inspired elastomer micro-fiber adhesives," in *Proc. IEEE/RSJ Int. Conf. Intell. Robots Syst.*, 2014, pp. 4624–4629.
- [16] H. Jiang et al., "A robotic device using gecko-inspired adhesives can grasp and manipulate large objects in microgravity," *Sci. Robot.*, vol. 2, no. 7, 2017, Art. no. eaan4545.
- [17] R. Chen, L. Wu, Y. Sun, J.-Q. Chen, and J.-L. Guo, "Variable stiffness soft pneumatic grippers augmented with active vacuum adhesion," *Smart Mater. Struct.*, vol. 29, no. 10, 2020, Art. no. 105028.
- [18] Z. Zhakypov, F. Heremans, A. Billard, and J. Paik, "An origami-inspired reconfigurable suction gripper for picking objects with variable shape and size," *IEEE Robot. Autom. Lett.*, vol. 3, no. 4, pp. 2894–2901, Oct. 2018.
- [19] M. Follador, F. Tramacere, and B. Mazzolai, "Dielectric elastomer actuators for octopus inspired suction cups," *Bioinspiration Biomimetics*, vol. 9, no. 4, 2014, Art. no. 046002.
- [20] H. Bing-Shan, W. Li-Wen, F. Zhuang, and Z. Yan-Zheng, "Bio-inspired miniature suction cups actuated by shape memory alloy," *Int. J. Adv. Robot. Syst.*, vol. 6, no. 3, pp. 151–160, 2009.
- [21] T. Takahashi, M. Suzuki, and S. Aoyagi, "Octopus bioinspired vacuum gripper with micro bumps," in *Proc. IEEE 11th Annu. Int. Conf. Nano/Micro Eng. Mol. Syst.*, 2016, pp. 508–511.
- [22] S. Baik, D. W. Kim, Y. Park, T.-J. Lee, S. H. Bhang, and C. Pang, "A wet-tolerant adhesive patch inspired by protuberances in suction cups of octopi," *Nature*, vol. 546, no. 7658, pp. 396–400, 2017.
- [23] T. M. Huh et al., "A multi-chamber smart suction cup for adaptive gripping and haptic exploration," in *Proc. IEEE Int. Conf. Intell. Robot. Syst.*, 2021, pp. 1786–1793.
- [24] Y. Yoo, J. Eom, M. Park, and K.-J. Cho, "Compliant suction gripper with seamless deployment and retraction for robust picking against depth and tilt errors," *IEEE Robot. Autom. Lett.*, vol. 8, no. 3, pp. 1311–1318, 2023, doi: [10.1109/LRA.2023.3238903](https://doi.org/10.1109/LRA.2023.3238903).
- [25] Y. Wang and R. Hensel, "Bioinspired underwater adhesion to rough substrates by cavity collapse of cupped microstructures," *Adv. Funct. Mater.*, vol. 31, no. 31, 2021, Art. no. 2101787.
- [26] Z. Xie et al., "Octopus arm-inspired tapered soft actuators with suckers for improved grasping," *Soft Robot.*, vol. 7, no. 5, pp. 639–648, 2020.
- [27] F. Tramacere, A. Kovalev, T. Kleinteich, S. N. Gorb, and B. Mazzolai, "Structure and mechanical properties of Octopus vulgaris suckers," *J. Roy. Soc. Interface*, vol. 11, no. 91, 2014, Art. no. 20130816.
- [28] C. Laschi, M. Cianchetti, B. Mazzolai, L. Margheri, M. Follador, and P. Dario, "Soft robot arm inspired by the octopus," *Adv. Robot.*, vol. 26, no. 7, pp. 709–727, 2012.
- [29] M. Cianchetti, A. Licofonte, M. Follador, F. Rogai, and C. Laschi, "Bioinspired soft actuation system using shape memory alloys," *Actuators*, vol. 3, no. 3, pp. 226–244, 2014.
- [30] Y. Asano et al., "Human mimetic musculoskeletal humanoid Kengoro toward real world physically interactive actions," in *Proc. IEEE-RAS Int. Conf. Humanoid Robots*, 2016, pp. 876–883.
- [31] E. Brown et al., "Universal robotic gripper based on the jamming of granular material," *Proc. Nat. Acad. Sci. USA*, vol. 107, no. 44, pp. 18809–18814, 2010.



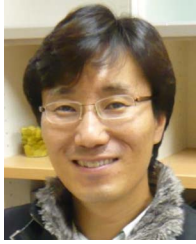
**Yong-Sin Seo** received the M.S. degree in mechanical engineering from Chungnam National University, Daejeon, South Korea, in 2019.

He is currently a Student Researcher with the Department of Robotics and Mechatronics, Korea Institute of Machinery and Materials, Daejeon, South Korea. His research interests include human-mimetic robot manipulator and soft pneumatic gripper for collaborative robot.



**Jae-Young Lee** received the M.S. degree in mechanical engineering from Chungnam National University, Daejeon, South Korea, in 2019. He is currently working toward the Ph.D. degree in mechanical engineering with Sungkyunkwan University, Suwon, South Korea.

Since 2017, he has been with the Department of Robotics and Mechatronics, Korea Institute of Machinery and Materials, Daejeon, South Korea. His research interests include soft robotics.



**Chanhun Park** received the M.S. degree from the Pohang University of Science and Technology, Pohang, South Korea, and the Ph.D. degree from the Korea Advanced Institute of Science and Technology, Daejeon, South Korea, in 1994, 1996, and 2010, respectively, both in mechanical engineering.

Since 1996, he has been a Principal Researcher with the Korea Institute of Machinery and Materials, Daejeon, South Korea. Since 2022, he has been the Head of AI Robot Research Division, Korea Institute of Machinery and Materials. His research interests include robot manipulator design and control, force-feedback control system, cooperative robot and its application, dexterous manipulators for industrial robotics, gripper systems for human-robot cooperation, and assembly process automation.



**Jongwoo Park** received the M.S. and Ph.D. degrees in control and instrumentation engineering from Korea University, Seoul, South Korea, in 2007 and 2016, respectively.

He is currently a Senior Researcher with the Department of Robotics and Mechatronics, Korea Institute of Machinery and Materials, Daejeon, South Korea. His research interests include analysis of robot control and integrative system, for robot, human hand motion.



**Byung-Kil Han** received the M.S. and Ph.D. degrees in mechanical engineering from the Korea Advanced Institute of Science and Technology, Daejeon, South Korea, in 2010 and 2019, respectively.

In 2013, he was a Research Intern with the Human-Computer Interaction Group, Microsoft Research Asia, Beijing. He is currently a Senior Researcher with the Korea Institute of Machinery and Materials, Daejeon, South Korea. His current research interests include haptics, 3-D vision, and deep learning-based robot manipulation.



**Je-Sung Koh** (Member, IEEE) received the B.S. and Ph.D. degrees in mechanical and aerospace engineering from Seoul National University, Seoul, South Korea, in 2008 and 2014, respectively.

He was a Postdoctoral Fellow with Harvard Microrobotics Laboratory until 2017. He is currently an Assistant Professor of mechanical engineering with Aju University, Suwon, South Korea. His research interests include biologically inspired small-scale robot design and soft robots.



**Uikyum Kim** (Member, IEEE) received the B.S. and Ph.D. degrees in mechanical engineering from Sungkyunkwan University, Suwon, South Korea, in 2011 and 2017, respectively.

He was a Senior Researcher with the Department of Robotics and Mechatronics, Korea Institute of Machinery and Materials, Daejeon, South Korea, until 2021. He is currently an Assistant Professor of mechanical engineering with Aju University, Suwon, South Korea. His research interests include robot hand, surgical robot, force/torque sensor, force/tactile sensors for robotics applications, haptic interfaces, force-feedback control system, dexterous manipulators for industrial robotics, soft sensor, and sensor calibration computing algorithms.



**Hugo Rodrigue** (Senior Member, IEEE) was born in Montreal, QC, Canada, in 1985. He received the B.Eng. degree in mechanical engineering from McGill University, Montreal, QC, Canada, in 2008, the M.S. degree in industrial engineering from Ecole Polytechnique de Montreal, Montreal, QC, Canada, in 2010, and the Ph.D. degree in mechanical and aerospace engineering from Seoul National University, Seoul, South Korea, in 2015.

He is currently an Assistant Professor with the School of Mechanical Engineering, Sungkyunkwan University, Seoul, South Korea. His research interests include soft actuation, smart materials, and soft robotics.



**Jeongae Bak** received the B.S. degree from the School of Mechanical Engineering, Hanyang University, Seoul, South Korea, and the Ph.D. degree in hovering control of an underwater robot from the School of Mechanical and Aerospace Engineering, Seoul National University, Seoul, South Korea, in 2014 and 2020, respectively.

She is currently a Senior Researcher with the Department of Robotics and Mechatronics, Korea Institute of Machinery and Materials, Daejeon, South Korea. Her current research interests include wearable robot and underwater robotic platform design and control.



**Sung-Hyuk Song** received the B.S. degree in physics from Korea University, Seoul, South Korea, in 2011, and the Ph.D. degree in mechanical and aerospace engineering from Seoul National University, Seoul, South Korea, in 2016.

He was a Research Fellow in regenerative medicine with Wake Forest Baptist Medical Center, Winston-Salem, NC, USA, in 2016. He is currently a Principal Researcher with the Department of Robotics and Mechatronics, Korea Institute of Machinery and Materials, Daejeon, South Korea. His research interests include soft robotics, universal gripper, soft morphing wheel, artificial muscle, 3-D printing in manufacturing, and manufacturing automation.